Nonequilibrated Counterpropagating Edge Modes in the Fractional Quantum Hall Regime

Anna Grivnin, Hiroyuki Inoue, Yuval Ronen, Yuval Baum, Moty Heiblum, Vladimir Umansky, and Diana Mahalu
Braun Center for Submicron Research, Department of Condensed Matter Physics, Weizmann Institute of Science, Rehovot 76100, Israel

(Received 15 September 2014; published 22 December 2014)

It is well established that density reconstruction at the edge of a two-dimensional electron gas takes place for hole-conjugate states in the fractional quantum Hall effect (such as $v = 2/3$, $3/5$, etc.). Such reconstruction leads, after equilibration between counterpropagating edge channels, to a downstream chiral current edge mode accompanied by upstream chiral neutral modes (carrying energy without net charge). Short equilibration length prevented thus far observation of the counterpropagating current channels—the hallmark of density reconstruction. Here, we provide evidence for such nonequilibrated counterpropagating current channels, in short regions ($l = 4$ μm and $l = 0.4$ μm) of fractional filling $v = 2/3$ and, unexpectedly, $v = 1/3$, sandwiched between two regions of integer filling $v = 1$. Rather than a two-terminal fractional conductance, the conductance exhibited a significant ascension towards unity quantum conductance ($G_Q = e^2/h$) at or near the fractional plateaus. We attribute this conductance rise to the presence of a nonequilibrated channel in the fractional short regions.

DOI: 10.1103/PhysRevLett.113.266803 PACS numbers: 73.43.Jn, 72.20.Ht, 73.23.Ad

Ever since the realization that current in quantum Hall systems is carried by chiraly flowing electrons near the edge of the two-dimensional electron gas (2DEG) [1,2], the study of edge dynamics has gained interest both theoretically and experimentally. While in the integer quantum Hall effect (IQHE) regime the picture of chiral edge channels is better understood, it is not the case in the fractional regime. It was suggested by Chang and Beenakker [3,4] that in the fractional quantum Hall effect (FQHE), very much like in the IQHE [5], the filling factor (density) decreases monotonically towards the edge of the electron gas, and the current is carried *downstream* by chiral channels in incompressible strips [3]. However, for hole-conjugate states, namely, $n + 1/2 < v < n + 1$, with $n = 0, 1, 2, \ldots$ (say, $\nu = 2/3$, $3/5$, etc.), MacDonald and Wen [6–8] proposed that the density profile near the edge is nonmonotonic (named, *reconstructed*). Such density profile is predicted to support multiple propagating (downstream) or counterpropagating (upstream) edge channels. For example, based on the hierarchical picture [9,10], the $v = 2/3$ state supports two counterpropagating chiral channels: a downstream electron channel, $v = 1$, and an upstream $v = 1/3$ channel—both were never observed [11]. Moreover, this picture suggests a two-terminal conductance $G = 4/3 \times e^2/h$ for the $v = 2/3$ state—also, not observed likely due to a short equilibration length between the channels. This motivated Kane *et al.* [12,13] and later Meir *et al.* [14,15] to propose equilibration among the edge channels due to interchannel Coulomb interaction accompanied by interchannel tunneling due to disorder. In the equilibrated state, there is a downstream $v = 2/3$ charged mode and an upstream neutral mode. The latter one was recently observed via shot noise measurements [16–18] and also by heating a narrow constriction [16,19–21]. Noting that for a sufficiently shallow confining potential near the edge, edge reconstruction was predicted to take place also in a variety of non-hole-conjugate fractional states [22–29] (neutral modes had been recently found in electronlike fractional states [18]) and even in integer fillings [30].

Our experiment was designed to study pre-equilibrated edge transport in the $v = 2/3$ and $v = 1/3$ states, by varying the propagation length. The channel's propagation length was defined by a short fractional region ranging $l = 0.4$–4 μm, being long enough to suppress tunneling, but on a typical scale of the single particle scattering length. Sample edges were defined by depleting metallic gates, which created a smooth edge potential. The fractional regions (with filling v_f) were induced by top gates, each being sandwiched between two regions with bulk filling $v_B = 1$ as drawn in Fig. 1. If a nonequilibrated edge channel in the fractional regions supports a downstream edge channel $v = 1$, the transmission coefficient through it could ideally (neglecting reflections at the boundaries) approach unity. However, if equilibration between the counterpropagating channels takes place in a fractional region, say, in the $v_f = 2/3$ region, then only $2/3$ of the injected current would be transmitted—as is always observed in macroscopic samples [31,32].

Samples were fabricated on a variety of GaAs-AlGaAs heterostructures embedding high-mobility 2DEG. The samples' boundaries were defined by wet etching and depleting metallic gates as shown in Fig. 1. Different width fractional regions (45 μm long denoted by LR, and

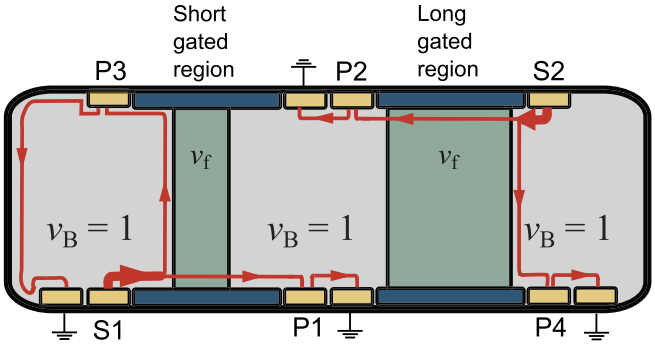

FIG. 1 (color online). Samples are fabricated in heterostructures embedding 2DEG with density 1.5×10^{11} cm^{-2} with mobility 6×10^6 cm^2 V^{-1} s^{-1} buried 85 nm below the surface. Each sample embeds two fractional regions, a long region (LR) of 45 μm and a short region (SR) of either 4 μm or 0.4 μm. Current is injected from the source contact S1 (S2), towards a short (long) top-gated fractional region. The filling of the fractional region is varied by applying negative bias to the gate (colored in dark green). The current flows along a defining gate (dark blue) negatively biased and depleted from electrons. The transmitted current is deduced from the measured voltage between $P1$ ($P2$) and the ground.

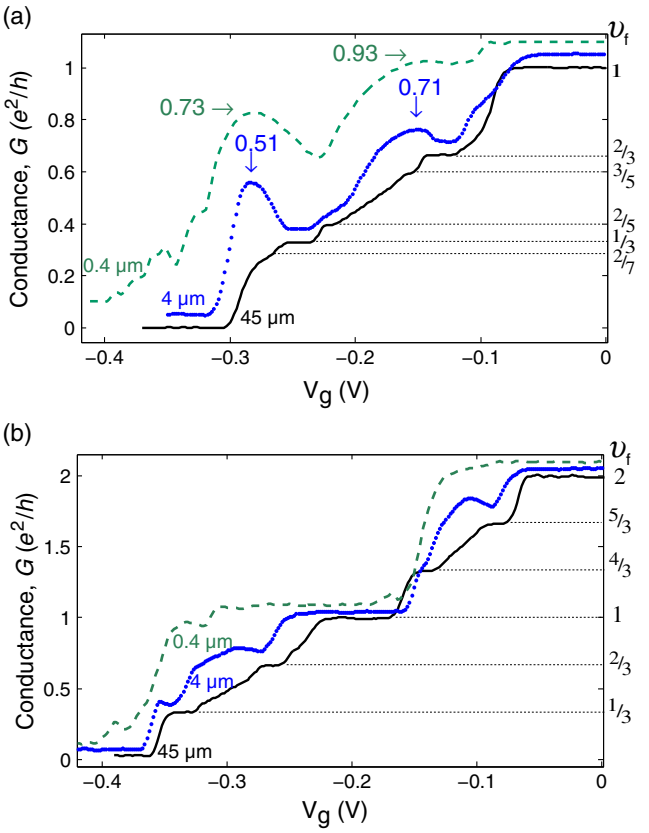

FIG. 2 (color online). Conductance vs top-gate voltage of three different fractional region sizes: long region (LR), 45 μm (black solid line); short region (SR), 4 μm (blue dotted line); and short region (SR), 0.4 μm (dark cyan dashed line). (a) Measurements performed at 8.5 T and bulk filling factor $\nu_B = 1$. The LR conductance shows a few fractional plateaus. For SR $= 4$ μm, the conductance near $\nu_f = 2/3$ rises up to $0.71 \times e^2/h$, and of SR $=$ 0.4 μm peaks at $0.93 \times e^2/h$. Similarly, the conductance near $\nu_f = 1/3$ peaks at $0.51 \times e^2/h$ for SR $= 4$ μm and $0.73 \times e^2/h$ for SR $= 0.4$ μm. Conductance plateaus at $\nu_f = 2/5$, $3/5$ and a signature of $\nu_f = 2/7$ also seen at LR. For $\nu_f = 2/5$, a reminiscent signature of reconstruction is also seen in the SR, while at $\nu_f = 3/5$, any signature is absorbed by the conductance peak of $\nu_f = 2/3$. The graphs are shifted by $0.05 \times e^2/h$ for convenience. (b) Similar measurements at 4.3 T at $\nu_B = 2$. Conductance of LR (black solid line) shows plateaus at values of $(2, 5/3, 4/3, 1, 2/3, 1/3) \times e^2/h$. The SR $= 4$ μm shows weaker conductance peaks near $(5/3, 2/3, 1/3)$ while around the integer value of $1 \times e^2/h$ the conductance is flat or monotonic, without peaks. For the SR $= 0.4$ μm, the conductance increases near all the fractional fillings but remains constant $1 \times e^2/h$ near $\nu_f = 1$.

0.1–4 μm long denoted by SR) were defined by top gates, which served to vary the electron density underneath. An ingrown n^+:GaAs layer, 1 μm below the 2DEG, served as a "back gate," allowing us to vary the electron density in the range 0.5–2.2×10^{11} cm^{-2}. The transmission through the fractional region was measured at different magnetic fields, at different electron densities, and at different temperatures. Current was injected at the source (S) with the voltage measured at the probes ($P1$ and $P2$). Within each sample, one SR and one LR were embedded, with LR allowing calibrating the gate voltage required for a certain filling underneath [with the depth of the 2DEG (85 nm), much smaller than the top-gate length; nearly equal capacitance per length was assumed for all gates' lengths]. Measurements were performed using a standard lockin technique with excitation voltage ~ 2 μV rms at 179 Hz at lattice temperature of 35 mK (unless stated otherwise). Note that the excitation energy and temperature were substantially lower than the presumed energy gaps of $\upsilon = 2/3$ and $\upsilon = 1/3$ ($\sim$350 μeV and higher) [33].

Our main results are summarized in Fig. 2(a)—at bulk filling $\upsilon_B = 1$, with electron density $n_B \sim 2.2 \times 10^{11}$ cm^{-2} and $B = 8.5$ T. The transmission (in units of the quantum conductance) from source $S1$ to probe $P1$ (through the sandwich $\upsilon_B = 1 - \upsilon_f < 1 - \upsilon_B = 1$) is shown as a function of the fractional region gate voltage. The transmission through LR (measured from source $S2$ to probe $P2$, solid black line) was used as reference of the filling factor beneath the gated regions. Conductance plateaus at $\upsilon_f = 2/3$ and $\upsilon_f = 1/3$ are clearly visible, with somewhat weaker ones at $\upsilon_f = 3/5$ and $\upsilon_f = 2/5$ (and a signature of $\upsilon_f = 2/7$). However, in structures with SR $= 4$ μm (dotted blue line) and 0.4 μm (dashed green line) the conductance is not monotonic—exceeding the corresponding quantized values, rising markedly at the lower density side of the two main fractional plateaus (overlapping lower lying plateaus, with even a weak sign near the $2/5$ plateau for

SR $= 4\ \mu$m). Note the large enhancement of the transmission for the SR $= 0.4\ \mu$m, approaching $0.93 \times e^2/h$ at $\nu_f = 2/3 - \nu_f = 3/5$, and $0.73 \times e^2/h$ near $\nu_f = 1/3$. Similar behavior was observed in other samples made from four differently grown heterostructures with carrier densities in the range of $(1.7\text{–}2.1) \times 10^{11}$ cm^{-2}, and with different SR lengths (see the Supplemental Material [34], Fig. S1). While the enhanced conductance at the hole-conjugate fractional fillings supports our hypothesis of nonequilibrated edge channels at small-enough propagation lengths, the observed enhancement in particlelike states is somewhat of a surprise—making the effect rather ubiquitous. However, it supports a proliferation of edge reconstruction points and presence of neutral modes, as indeed was recently observed [18].

Since upstream neutral modes were not observed in the integer regime, multiple nonequilibrated edge channels are not expected [35–40]. Having this in mind, we repeated the experiments with SR in the integer regime, namely, $\nu_f =$ integer: The bulk filling was set at $\nu_B = 2$ ($B = 4.3$ T and density 2.2×10^{11} cm^{-2}) with the gated region tuned continuously from $\nu_f = 2$ to $\nu_f = 0$. The measured conductance vs gate voltage is shown in Fig. 2(b). The transmission through the LR shows multiple plateaus at $(2, 5/3, 4/3, 1, 2/3, 1/3) \times e^2/h$, with the transmission through the SR being nonmonotonic, with clear conductance peaks only near the fractional fillings $\nu_f = 5/3$, $2/3$, and $1/3$—but not around $\nu_f = 1$. At a lower magnetic field ($B = 2.8$ T, and correspondingly lower density 1.4×10^{11} cm^{-2}), when fractional states are not observed, the conductance through all lengths of SR declined monotonically, showing only the plateaus of $2e^2/h$ and $1e^2/h$ (see the Supplemental Material [34], Fig. S2).

Edge reconstruction, being an outcome of electron interaction in a confining potential, is expected to depend on electron density and external magnetic field. By fixing the density at $n_B \sim 2.0 \times 10^{11}$ cm^{-2}, transmission measurements were repeated at three different magnetic fields, $B = 8.5$ T, 7.7 T, and 7.0 T, within the range of $\nu_B = 1$ conductance plateau. The conductance is plotted for LR $= 45\ \mu$m and SR $= 0.4\ \mu$m in Fig. 3(a) [data for SR $= 4\ \mu$m are shown in the Supplemental Material [34], Fig. S3(a)]. While there was no visible effect in the LR sample, the transmission peak in the SR region tended to increase as the magnetic field was lower. Next, the magnetic field was fixed at $B = 7$ T and the density was varied by charging the back gate in the range $n_B = 1.7\text{–}2.0 \times 10^{11}$ cm^{-2}, again within the range of $\nu_B = 1$ conductance plateau. Here, aside from the shift in the pinch off voltage, the conductance of LR $= 45\ \mu$m and SR $= 0.4\ \mu$m effectively remained unaltered [see Fig. 3(b), with data of SR $= 4\ \mu$m, and the Supplemental Material [34], Fig. S3(b)].

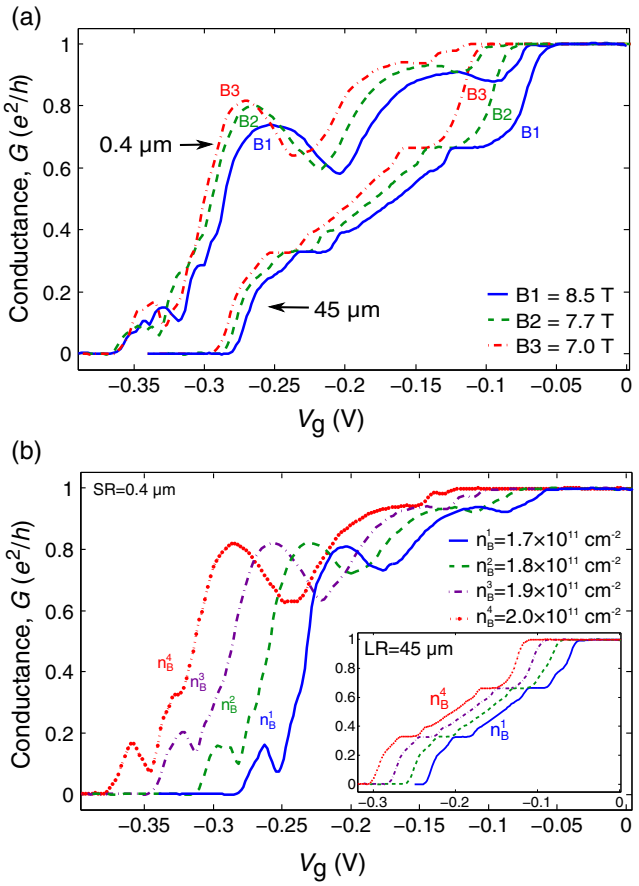

FIG. 3 (color online). Dependence of conductance on magnetic field and electron density. (a) Conductance of LR $= 45\ \mu$m and of SR $= 0.4\ \mu$m as a function of the top-gate voltage at different magnetic fields $B = (8.5, 7.7, 7.0)$ T, drawn in blue (solid line), green (dashed line), and red (dash-dotted line), respectively. As the magnetic field decreases, the conductance near $\nu_f = 1/3, 2/3$ rises slightly. Similar behavior was observed for SR $= 4\ \mu$m (see the Supplemental Material [34]). (b) Conductance of LR $= 45\ \mu$m (inset) and of SR $= 0.4\ \mu$m as function of the top-gate voltage at $B = 7$ T and at different bulk densities of $n_B = (1.7, 1.8, 1.9, 2) \times 10^{11}$ cm^{-2}, corresponding to different bias of the back gate, (0.4, 0.6, 0.8, 1.0) V, drawn in blue (solid line), green (dashed line), purple (dash-dotted line), and red (dotted line), respectively. The conductance peaks for $\nu_f = 1/3$, $2/3$ remain nearly unchanged.

Temperature dependence was measured in order to rule out tunneling or activated transport through the narrow SR. With increasing temperature, the nonmonotonic conductance peak near the fractional plateaus slightly diminished [Fig. 4(a)], suggesting an enhanced interchannel tunneling and thus suppressing the equilibration length [26,41]. On the other hand, the transmission through SR $= 0.4\ \mu$m in the integer regime ($B = 2.8$ T) was found to increase steadily as shown in Fig. 4(b), starting already at $T = 230$ mK. The conductance at 4 K is plotted for reference in dash-dotted line (data of SR $= 4\ \mu$m; see [34], Figs. S5 and S6).

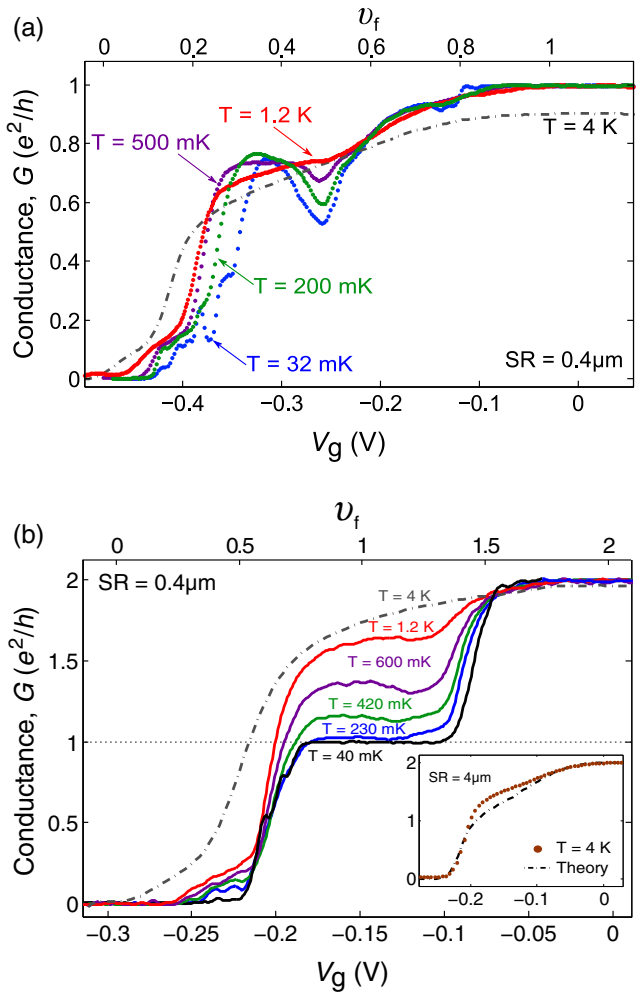

FIG. 4 (color online). Temperature dependence of SR $= 0.4$ μm, 30 mK–4.2 K at $\nu_B = 1$ and $\nu_B = 2$. The bottom x axis denotes the voltage on the top gate, the top x axis is the corresponding filling factor ν_f at SR. (a) Conductance of SR $= 0.4$ μm as a function of top-gate voltage at different temperatures (32 mK, 200 mK, 500 mK, 1.2 K, 4.2 K). The apparent conductance peaks near $\nu_f = 1/3$, $2/3$ decay as temperature rises, with that of the $\nu_f = 1/3$ being much more prominent. (b) Similar conductance measurements at $\nu_B = 2$ with temperature range of 40 mK, 420 mK, 600 mK, 1.2 K, 4.2 K. As temperature increases throughout the sample, the transmitted current in $\nu_f = 1$ rises due to increase of electron tunneling through the gated regions, as expected. Inset: comparison of the classical simulation and the high temperature measurement at SR $= 4$ μm—being qualitatively similar.

Can the observed nonmonotonic dependence of the transmission through the fractional regime be explained by a classical estimate of bulk currents in the Hall regime? In order to clarify that possibility, we described the system by a standard Hall matrix in each of the regions, $\upsilon_B = 1$ and $\upsilon_f < 1$, assuming a small longitudinal conductivity (R_{xx}) in each region. Solving the Poisson equation with the appropriate boundary conditions, we calculated the transmitted currents across the SR region as a function of its (classical) filling factor. The solution of the classical equations for SR $= 4$ μm coincides with the behavior of the conductance in the integer regime at $T \sim 4$ K, namely, when the QHE plateaus vanish [inset in Fig. 4(b)], justifying this approximation. When we compare the measured results in the fractional regime, say, at $\nu_f = 1/3$ and at $\nu_f = 2/3$, the conductance peaks are well *above* the calculated conductance (for more details, see the Supplemental Material [34], Sec. IV). Though the numerical analysis leads to the same conclusion for SR < 1 μm, it is highly sensitive to changes in the spatial discretization scheme, and thus less reliable.

The observation of nonequilibrated current channels reveals the complexity and multiplicity of chiral channels transport in the FQHE, and distinguishes it from transport in the IQHE regime. In a recent work, we reported the proliferation of neutral modes in many fractional states (upstream along the edge and diffusively throughout the incompressible bulk) [18]—making edge reconstruction as a source of such neutral modes rather prevalent. The present observation brings to light the direct source of the equilibrated neutral modes, which is generally concealed in most measurements. Our observation, of an increased transmission of integer channels through fractional ones—described here in some detail for $\nu_f = 2/3$ and $1/3$, and also in $\nu_f = 2/5$, $4/5$, and $5/3$—suggests edge reconstruction at these fractions, with an increase carrier density towards higher filling—likely $\upsilon = 1$, or a lower-lying filling—near the edge of the sample. As it is now clear that neutral modes persist throughout the fractional quantum Hall regime (hence, being likely to inhibit interference of fractional charges [42]), their weakening (or elimination) by sample design is desirable for the study anyonic statistics in the fractional regime [43].

We thank Ady Stern, Yuval Gefen, and Yigal Meir for useful discussions. We acknowledge the partial support of the Israeli Science Foundation (ISF), the Minerva Foundation, the U.S.-Israel Bi-National Science Foundation (BSF), the European Research Council under the European Community's Seventh Framework Program (FP7/2007-2013)/ERC, Grant No. 227716, and the German Israeli Project Cooperation (DIP).

[1] S. Das Sarma and A. Pinczuk, *Perspectives in Quantum Hall Effects* (Wiley, New York, 2007).
[2] X. G. Wen, Phys. Rev. B **41**, 12838 (1990).
[3] C. W. J. Beenakker, Phys. Rev. Lett. **64**, 216 (1990).
[4] A. M. Chang and J. E. Cunningham, Solid State Commun. **72**, 651 (1989).
[5] B. I. Halperin, Phys. Rev. B **25**, 2185 (1982).
[6] A. H. MacDonald, Phys. Rev. Lett. **64**, 220 (1990).
[7] M. D. Johnson and A. H. MacDonald, Phys. Rev. Lett. **67**, 2060 (1991).
[8] X. G. Wen, Phys. Rev. B **43**, 11025 (1991).
[9] F. D. M. Haldane, Phys. Rev. Lett. **51**, 605 (1983).

[10] B. Halperin, Phys. Rev. Lett. **52**, 2390 (1984).
[11] R. C. Ashoori, H. L. Stormer, L. N. Pfeiffer, K. W. Baldwin, and K. West, Phys. Rev. B **45**, 3894 (1992).
[12] C. L. Kane, M. P. A. Fisher, and J. Polchinski, Phys. Rev. Lett. **72**, 4129 (1994).
[13] C. L. Kane and M. P. A. Fisher, Phys. Rev. B **51**, 13449 (1995).
[14] Y. Meir, Phys. Rev. Lett. **72**, 2624 (1994).
[15] J. Wang, Y. Meir, and Y. Gefen, Phys. Rev. Lett. **111**, 246803 (2013).
[16] A. Bid, N. Ofek, H. Inoue, M. Heiblum, C. L. Kane, V. Umansky, and D. Mahalu, Nature (London) **466**, 585 (2010).
[17] M. Dolev, Y. Gross, R. Sabo, I. Gurman, M. Heiblum, V. Umansky, and D. Mahalu, Phys. Rev. Lett. **107**, 036805 (2011).
[18] H. Inoue, A. Grivnin, Y. Ronen, M. Heiblum, V. Umansky, and D. Mahalu, Nat. Commun. **5**, 4067 (2014).
[19] Y. Gross, M. Dolev, M. Heiblum, V. Umansky, and D. Mahalu, Phys. Rev. Lett. **108**, 226801 (2012).
[20] I. Gurman, R. Sabo, M. Heiblum, V. Umansky, and D. Mahalu, Nat. Commun. **3**, 1289 (2012).
[21] V. Venkatachalam, S. Hart, L. Pfeiffer, K. West, and A. Yacoby, Nat. Phys. **8**, 676 (2012).
[22] L. Brey, Phys. Rev. B **50**, 11861 (1994).
[23] D. B. Chklovskii, Phys. Rev. B **51**, 9895 (1995).
[24] M. Ferconi, M. R. Geller, and G. Vignale, Phys. Rev. B **52**, 16357 (1995).
[25] E. V. Tsiper and V. J. Goldman, Phys. Rev. B **64**, 165311 (2001).
[26] X. Wan, K. Yang, and E. H. Rezayi, Phys. Rev. Lett. **88**, 056802 (2002).
[27] X. Wan, E. H. Rezayi, and K. Yang, Phys. Rev. B **68**, 125307 (2003).
[28] K. Yang, Phys. Rev. Lett. **91**, 036802 (2003).
[29] Y. N. Joglekar, H. K. Nguyen, and G. Murthy, Phys. Rev. B **68**, 035332 (2003).
[30] C. deC. Chamon and X. G. Wen, Phys. Rev. B **49**, 8227 (1994).
[31] L. P. Kouwenhoven, B. J. van Wees, N. C. van der Vaart, C. J. P. M. Harmans, C. E. Timmering, and C. T. Foxon, Phys. Rev. Lett. **64**, 685 (1990).
[32] B. W. Alphenaar, J. G. Williamson, H. van Houten, C. W. J. Beenakker, and C. T. Foxon, Phys. Rev. B **45**, 3890 (1992).
[33] R. R. Du, H. L. Stormer, D. C. Tsui, L. N. Pfeiffer, and K. W. West, Phys. Rev. Lett. **70**, 2944 (1993).
[34] See Supplemental Material at http://link.aps.org/supplemental/10.1103/PhysRevLett.113.266803 for additional measurements and theory supporting our observation described in this Letter.
[35] R. J. Haug, A. H. MacDonald, P. Streda, and K. von Klitzing, Phys. Rev. Lett. **61**, 2797 (1988).
[36] S. Washburn, A. B. Fowler, H. Schmid, and D. Kern, Phys. Rev. Lett. **61**, 2801 (1988).
[37] S. Komiyama, H. Hirai, S. Sasa, and S. Hiyamizu, Phys. Rev. B **40**, 12566 (1989).
[38] J. M. Ryan, N. F. Deutscher, and D. K. Ferry, Phys. Rev. B **47**, 16594 (1993).
[39] H. Hirai, S. Komiyama, S. Sasa, and T. Fujii, Solid State Commun. **72**, 1033 (1989).
[40] P. L. McEuen, A. Szafer, C. A. Richter, B. W. Alphenaar, J. K. Jain, A. D. Stone, R. G. Wheeler, and R. N. Sacks, Phys. Rev. Lett. **64**, 2062 (1990).
[41] S. Komiyama, H. Hirai, M. Ohsawa, Y. Matsuda, S. Sasa, and T. Fujii, Phys. Rev. B **45**, 11085 (1992).
[42] M. Goldstein (unpublished).
[43] J. K. Jain, S. A. Kivelson, and D. J. Thouless, Phys. Rev. Lett. **71**, 3003 (1993).